Madencilik, 2020, 59(2), 93-100 *Mining, 2020, 59(2), 93-100*

BİLİMSEL madencilik DERGİSİ
SCIENTIFIC MINING JOURNAL
TMMOB Maden Mühendisleri Odası Yayını / *The Publication of the Chamber of Mining Engineers of Turkey*

Orijinal Araştırma / *Original Research*

DISSOLUTION PROPERTIES OF A DOLOMITE CONTAINING ZINC ORE IN SODIUM HYDROXIDE SOLUTIONS

DOLOMİT İÇEREN BİR ÇİNKO CEVHERİNİN SODYUM HİDROKSİT ÇÖZELTİLERİNDEKİ ÇÖZÜNME ÖZELLİKLERİ

Cavit Kumaş[a,*], İlhan Ehsani[a,**], Abdullah Obut[a,***]

[a] Hacettepe University, Mining Engineering Department, Ankara, TURKEY

Geliş Tarihi / *Received* : 04 Şubat / *February 2020*
Kabul Tarihi / *Accepted* : 30 Nisan / *April 2020*

Anahtar Sözcükler:
Alkaline leaching,
Dolomite,
Sodium hydroxide,
Smithsonite,
Zinc carbonate ore.

ABSTRACT

In this work, the dissolution properties of a dolomite containing zinc carbonate (smithsonite) ore sample having 24.22% ZnO were determined in sodium hydroxide solutions using X-ray diffraction (XRD), Fourier-transform infrared spectroscopy (FT-IR), thermal (TG/DTA) and chemical analyses methods. It was observed that the dissolution efficiency value of zinc continuously increased with the increase of sodium hydroxide concentration from 1 to 4 M and the highest zinc dissolution efficiency of 70.7% was reached after dissolution in 4 M NaOH solution at temperature of 298 K. The XRD, FT-IR, TG/DTA and chemical analyses of undissolved solids obtained after dissolution of ore sample in 4 M NaOH solution at 298 K revealed that the smithsonite phase in the sample completely dissolved whereas the main gangue mineral dolomite remained practically unaffected, showing the selectivity of sodium hydroxide solution considering zinc dissolution. Although the smithsonite phase in the sample totally dissolved, hundred percent zinc dissolution efficiency could not be reached, which may indicate the presence of zinc in the gangue components, i.e. dolomite, clay minerals etc., of the studied ore sample.

Keywords:
Alkali liç,
Dolomit,
Sodyum hidroksit,
Simitsonit,
Çinko karbonat cevheri.

ÖZ

Bu çalışmada, dolomit içeren bir çinko karbonat (simitsonit) cevher numunesinin (%24,22 ZnO) sodyum hidroksit çözeltilerindeki çözünme özellikleri X-ışını kırınımı (XRD), Fourier dönüşümlü kızılötesi spektroskopisi (FT-IR), ısıl (TG/DTA) ve kimyasal analiz yöntemleri kullanılarak belirlenmiştir. Sodyum hidroksit derişiminin 1'den 4 M'ye artırılmasıyla çinko çözünme verimi değerinin sürekli olarak arttığı gözlenmiş ve %70,7'lik en yüksek çinko çözünme verimine 298 K sıcaklıktaki 4 M NaOH çözeltisinde yapılan çözme işlemi sonrasında ulaşılmıştır. Cevher numunesinin 298 K'deki 4 M NaOH çözeltisinde çözündürülmesi sonrasında elde edilen çözünmemiş katıların XRD, FT-IR, TG/DTA ve kimyasal analizleri, numune içindeki simitsonit fazının tamamen çözündüğü halde ana gang minerali dolomitin büyük ölçüde çözünmeden kaldığını ortaya çıkarmakta, bu durum da çinko çözünmesi dikkate alındığında sodyum hidroksit çözeltisinin seçiciliğini göstermektedir. Numunedeki simitsonit fazının tümünün çözünmesine rağmen yüzde yüz çinko çözünme verimine ulaşılamaması, çalışılan cevher numunesi içinde bulunan dolomit, kil mineralleri vb. gibi gang bileşenlerindeki muhtemel çinko varlığını işaret etmektedir.

* Sorumlu yazar / *Corresponding author:* cavit.kumas@hacettepe.edu.tr • https://orcid.org/0000-0002-4221-3034
** ilhan.ehsani@hacettepe.edu.tr • https://orcid.org/0000-0001-9741-8777
*** aobut@hacettepe.edu.tr • http://orcid.org/0000-0003-2979-322X

INTRODUCTION

Other than the sulfide ore deposits of zinc, there are several nonsulfide zinc ore deposits distributed around the world as a candidate for the primary production of zinc. But the conventional mineral processing techniques cannot efficiently be used for concentrating the nonsulfide ores in comparison to sulfide ores and extractive metallurgical processes (e.g. leaching) could be used for the obtainment of zinc from the nonsulfide ores. In the literature, there are many studies on leaching of dolomite and/or calcite containing smithsonite ores in different inorganic-organic acid (Dhawan et al., 2011; Ghasemi and Azizi, 2017) and alkaline solutions (Mujahed, 1966; Feng et al., 2007; Ghasemi and Azizi, 2018; Ehsani et al., 2019). Sodium hydroxide and ammoniacal solutions are the most studied reagents for alkaline leaching of zinc in nonsulfide ores because of their higher selectivity; i.e. in a zinc containing ore, the mineral smithsonite ($ZnCO_3$) easily dissolves while the main gangue minerals dolomite ($CaMg(CO_3)_2$), calcite ($CaCO_3$) and/or goethite (FeOOH) do not dissolve. In addition, electrowinning of zinc was claimed to be less energy consuming in sodium hydroxide solutions in comparison to acidic leaching solutions (Frenay, 1985; Zhao and Stanforth, 2000; DPT, 2001; Hitzman et al., 2003; Ju et al., 2005; Hosseini and Forssberg, 2009; Abkhoshk et al., 2014; Ejtemaei et al., 2014; Ghasemi and Azizi, 2018).

Although several chemically and mineralogically different zinc carbonate ore deposits are present in Turkey, the studies related with the dissolution properties of zinc from these sources using sodium hydroxide solution as the leaching reagent are scarce. Therefore, in this work, the dissolution properties of a dolomite and smithsonite containing zinc ore sample (from Kayseri, Turkey) in aqueous sodium hydroxide solutions were investigated with use of XRD, FT-IR, TG/DTA and chemical analyses in order to add new, detailed and comparative data into the relevant literature.

1. MATERIALS AND METHODS

In the experimental work, a ground smithsonite ore sample having 80% passing size of 127.1 µm was used (Figure 1). In addition to the main chemical components (Table 1), the sample also contained 0.65% K_2O, 0.62% Pb and 0.02% S. The XRD pattern, TG/DTA curves, FT-IR spectrum and chemical composition of ore sample indicated that the sample is a nonsulfide zinc ore sample and contains smithsonite and dolomite as the main phases. The sample also contains quartz, calcite, clay minerals and goethite in lesser amounts.

In this study, for comparison purposes, the experimental methods used in Ehsani et al. (2019) were followed. Briefly, the dissolution process was started by the addition of calculated amounts of sample to an aqueous sodium hydroxide solution (1, 2, 3 and 4 M NaOH) inside the reactor and continued for one hour under constant stirring at 298 K. After completion of one hour, the undissolved solids were filtrated under vacuum, water-washed, dried, weighed and analyzed in order to reveal the dissolution properties of zinc from the studied ore sample. In some of the experiments, different dissolution temperature, NaOH concentration and dissolution times were also tested. The solid/liquid ratio (0.15 kg dry ore/L solution) was also kept constant according to Ehsani et al. (2019), who investigated the leaching behaviour of zinc from a different smithsonite ore sample (29.16% ZnO, 6.75% SiO_2, 26.51% Fe_2O_3, 7.37% CaO, 1.92% Pb, 0.50% MgO) containing goethite and calcite as the main gangue minerals in sodium hydroxide solutions. In addition to zinc, for some of experiments, dissolution efficiencies of lead were also determined.

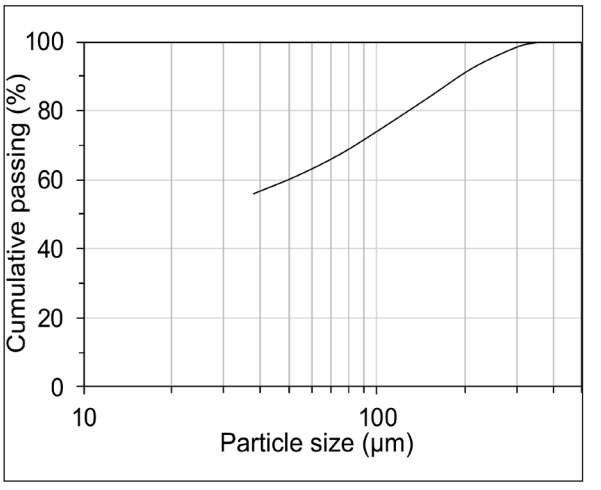

Figure 1. Particle size distribution of ore sample

Table 1. Main components (%) of ore sample

ZnO	24.22	SiO_2	12.30
Fe_2O_3	10.78	CaO	10.09
MgO	6.38	Al_2O_3	5.90
L.O.I.*	28.30		

*Loss on ignition

2. RESULTS AND DISCUSSION

The effect of sodium hydroxide concentration on the dissolution efficiencies of zinc and lead at different temperatures was given in Figure 2. As can be seen from Figure 2, dissolution efficiencies of zinc continuously increased with increasing NaOH concentration due to formation of soluble zincate type species in solution phase. Figure 2 also showed that the increase in dissolution efficiency of zinc at 298 K slowed down over 3 M NaOH concentration and reached 70.7% after dissolution in 4 M NaOH solution. This dissolution efficiency value of zinc, although varied according to mineralogies and chemical compositions of the samples studied and the experimental conditions applied, was close to the values obtained in the related literature (e.g., Frenay, 1985; Zhao and Stanforth, 2000; Ehsani et al. 2019) using ≥4 M NaOH solutions. For example, Ehsani et al. (2019) attained zinc dissolution efficiencies of 3.8%, 46.0%, 70.1% and 70.9% in 1 M, 2 M, 3 M and 4 M NaOH solutions, respectively, at 298 K. On the other hand, dissolution efficiencies of lead (Figure 2) were observed to be consistently increasing with increasing sodium hydroxide concentrations at both temperatures and reached highest values of 61.2% and 69.7% after dissolution in 4 M NaOH solution at 298 K and 363 K, respectively.

The dissolution efficiency values of zinc obtained at temperature of 363 K in comparison to the efficiencies obtained at 298 K were lower because of the increasing tendency of conversion of soluble zincate type species into solid zinc oxide at higher temperatures (Debiemme-Chouvy and Vedel, 1991; Uekawa et al., 2004; Moezzi et al., 2011). But, this conversion gradually lost its effectiveness at increasing NaOH concentrations, as observed by the steadily decreased difference between the dissolution efficiencies of zinc obtained at 298 K and at 363 K (Figure 2), and the lowered XRD (Rigaku, CuKa) peak intensities of zinc oxide found at 2θ(°) values of 31.78, 34.46, 36.28 and 47.52 (see Figure 3B). On the other hand, a separate dissolution experiment performed in highly concentrated 8 M NaOH solution showed that higher dissolution efficiencies of both zinc and lead were obtained after dissolution at 363 K (80.2% Zn and 78.3% Pb) in comparison to 298 K (75.5% Zn and 69.6% Pb).

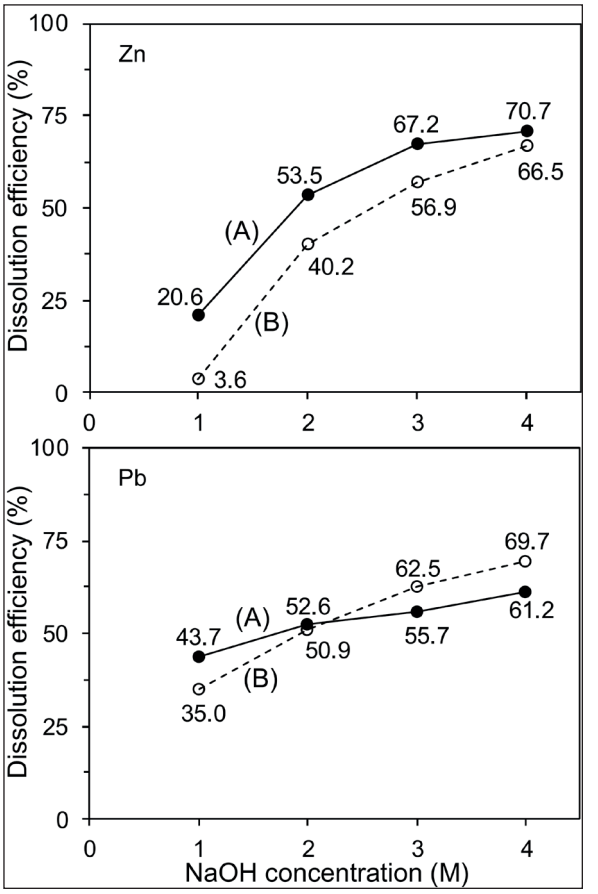

Figure 2. Effect of sodium hydroxide concentration on dissolution efficiencies of zinc and lead at (A) 298 K and (B) 363 K

The increase in dissolution of smithsonite phase in the sample with increased NaOH concentrations at 298 K could easily be followed by the decreases in intensities of the main XRD peaks of smithsonite observed at 2θ(°) values of 25.10, 32.60, 38.72, 42.86, 46.68 and 53.76 in the patterns of undissolved solids (Figure 3A). Up to 3 M NaOH concentration, XRD peak intensities of smithsonite phase continually decreased and after dissolution in 4 M NaOH solution, all of the peaks belonging to smithsonite

phase disappeared, indicating total dissolution of smithsonite in the sample at 298 K.

As mentioned before, due to conversion of zincate type species into zinc oxide at 363 K, main XRD peaks of ZnO could easily be observed in the patterns of undissolved solids obtained especially after dissolution in 1 M NaOH solution at 363 K (Figure 3B). For dissolution temperatures of both 298 K and 363 K, XRD peak intensities of dolomite practically did not change after dissolution in 1-4 M NaOH solutions, substantiating the selectivity of sodium hydroxide solutions considering zinc dissolution from the studied dolomite containing smithsonite ore sample.

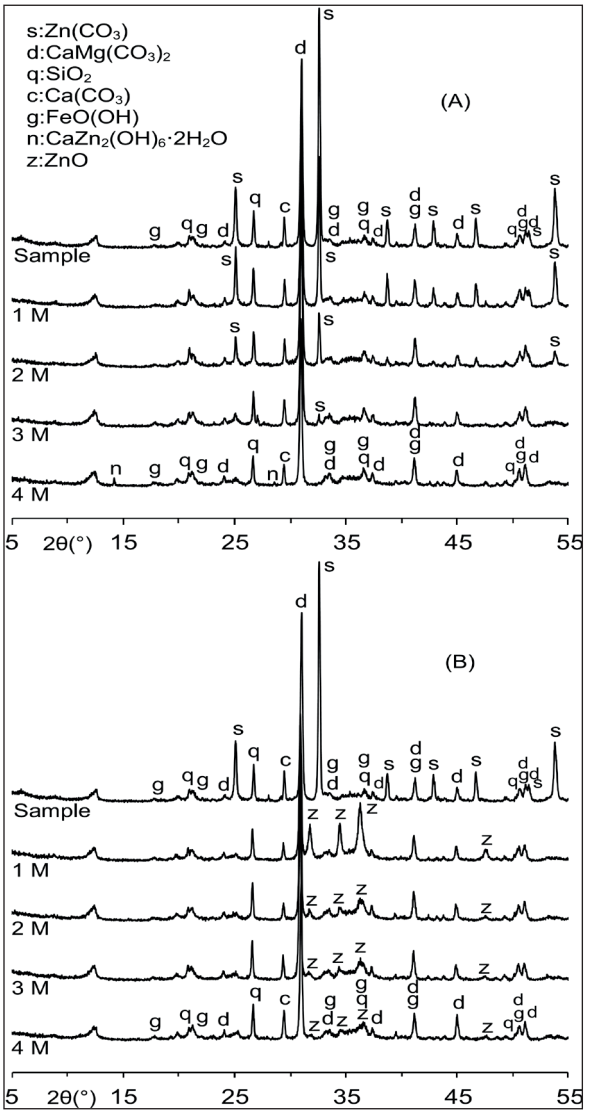

Figure 3. XRD patterns of ore sample and the undissolved solids obtained after dissolution in 1-4 M NaOH solutions at (A) 298 K and (B) 363 K

On the other hand, there were low intensity XRD peaks of hydrated Ca zincate ($CaZn_2(OH)_6 \cdot 2H_2O$) in the pattern of undissolved solids obtained after dissolution in 4 M NaOH solution (Figure 3A) and decelaration in dissolution efficiency of zinc at this concentration probably be related with formation of solid hydrated Ca zincate during dissolution. It was also observed that when dissolution time was increased to 4 hours in 3 M NaOH solution at 298 K (Figure 4), dissolution efficiency of zinc slightly reduced after second hour from 68.2% to 63.0%, probably due to the increased formation of solid hydrated Ca zincate phase, as also observed in the study of Ehsani et al. (2019), in which calcite is main Ca-bearing gangue and the decrease in zinc dissolution efficiency after second hour was higher, from 70.7% to 60.6%. Although the calcite containing ore sample studied by Ehsani et al. (2019) contained lower amounts of CaO (7.37%) than the dolomite containing ore sample (10.09% CaO) with minor calcite studied in this work, higher decrease in zinc dissolution efficiency associated with formation hydrated Ca zincate was observed for the calcite containing sample. This situation may suggest that formation of hydrated Ca zincate phase was faster in presence of calcite rather than dolomite, which in the first place should convert into calcite, as mentioned in the related literature (Gillott, 1964; Wang and Wainwright, 1986).

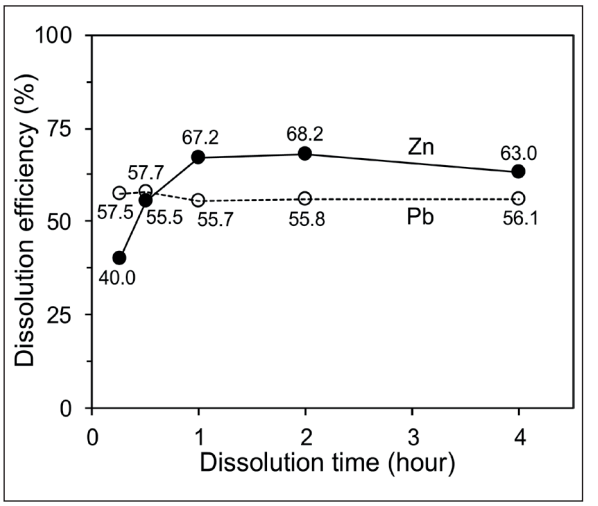

Figure 4. Effect of dissolution time on dissolution efficiencies of zinc and lead in 3 M NaOH solution at 298 K

In addition to XRD analyses, the dissolution of smithsonite in the sample was also followed by FT-IR and TG/DTA analyses. The FT-IR (Perkin Elmer, KBr pellet method) spectra of undissolved solids obtained after dissolution of ore sample in 1-4 M NaOH solutions at 298 K (Figure 5A) showed that the most distinctive absorption peak of smithsonite at 744 cm^{-1} (Huang and Kerr, 1960; Weir and Lippincott, 1961; Adler and Kerr, 1963) gradually lost its intensity at increasing NaOH concentrations and it completely disappeared when the concentration of solution became 4 M, indicating again total dissolution of smithsonite in the ore sample. The broad absorption peak of carbonate groups at 1436 cm^{-1} (Huang and Kerr, 1960; Weir and Lippincott, 1961; Adler and Kerr, 1963) in the spectrum of sample observed at higher wavenumber, 1439 cm^{-1}, in the spectra of undissolved solids, which may also be considered as an indication of dissolution of smithsonite in the ore sample. As also observed by XRD analyses, the absorption peak at 744 cm^{-1} belonging to smithsonite was not seen in the spectra of undissolved solids obtained after dissolution in NaOH solutions at 363 K (Figure 5B). For both dissolution temperatures and studied NaOH concentrations, presence of characteristic peak of dolomite at 729 cm^{-1} in the spectra of undissolved solids (Figure 5A-5B) indicated that dolomite was resistant to dissolution and remained in the undissolved solids.

The major indicator in DTA (Setaram Labsys, heating rate: 10°/min) curves (Figure 6) of the sample and the undissolved solids showing dissolution of smithsonite was the disappearance of endothermic peak at 660 K belonging to smithsonite decomposition (Zhang et al., 2013). The corresponding decreases in weight loss values belonging to this decomposition could also be seen in related TG curves of the sample and undissolved solids (Figure 6). Other endothermic peaks in DTA curves of undissolved solids about 570 K, 760 K and between 1000-1150 K may be attributed to goethite, clay minerals and dolomite (and minor calcite) (Grim and Rowland, 1942; Cuthbert and Rowland, 1947; Hurlbut, 1957; Frost et al., 2003), respectively, which indicated again that gangue minerals in the sample were resistant to dissolution in sodium hydroxide solutions.

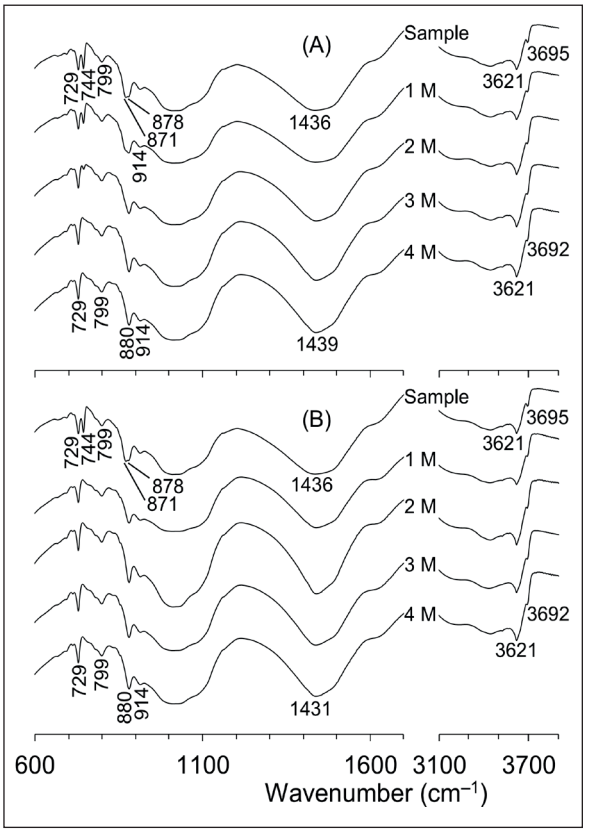

Figure 5. FTIR spectra of ore sample and the undissolved solids obtained after dissolution in 1-4 M NaOH solutions at (A) 298 K and (B) 363 K

Although the smithsonite phase in the sample having 24.22% ZnO was completely dissolved (see Figures 3, 5 and 6), the undissolved solids obtained after dissolution in 4 M NaOH solution at 298 K contained 9.73% ZnO. In order to find out the approximate dissolution efficiency limit of zinc in NaOH solutions at 298 K and the possible sources of undissolved zinc in the ore sample, two separate dissolution experiments were performed at 298 K under similar experimental conditions. The first experiment was performed in highly concentrated 8 M NaOH solution and dissolution efficiency of 75.5% Zn (69.6% Pb) was obtained, where undissolved solids contained 8.50% ZnO. In addition, the gangue minerals, dolomite, quartz, goethite and clay minerals, although affected some degree, still remained undissolved (Figure 7A). The second experiment was performed in approximately 4 M hydrochloric acid solution and the obtained dissolution efficiency of zinc was 94.9% (83.0% Pb), where the undissolved solids

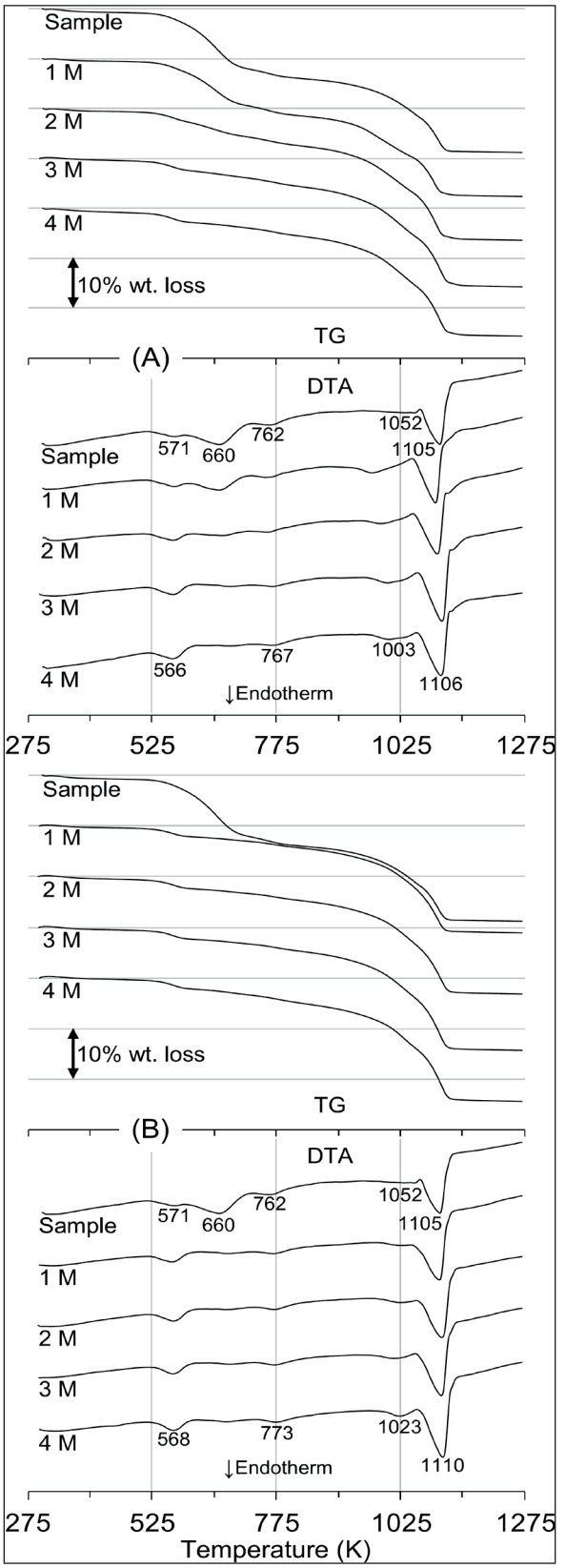

Figure 6. TG and DTA curves of ore sample and the undissolved solids obtained after dissolution in 1-4 M NaOH solutions at (A) 298 K and (B) 363 K

contained only 3.62% ZnO (When concentration of HCl increased to about 5 M, zinc dissolution efficiency only slightly increased (95.4% Zn and 83.1% Pb) and ZnO content of undissolved solids decreased to 3.30%.). For acid dissolution, quartz stayed unaffected, goethite seemed mostly unaffected and peak intensities of clay minerals lowered, whereas the carbonates, smithsonite, dolomite and minor calcite, in the sample totally dissolved, confirmed by the disappearance of strongest smithsonite (2θ=32.60°), dolomite (2θ=31.04°) and calcite (2θ=29.46°) peaks in the XRD pattern of undissolved solids (Figure 7B).

The difference between 100% zinc dissolution efficiency and dissolution efficiencies obtained in NaOH and HCl solutions probably be caused by the presence of zinc, other than in smithsonite, in structures of minerals of ore sample having some resistance to dissolution both in alkaline and acid solutions, i.e. zinc containing dolomite, clay minerals, goethite and calcite, as also indicated in the related literature (Whittaker and Żabiński, 1981; Rosenberg and Champness, 1989; Borg et al., 2003; Boni et al., 2009a,b; Coppola et al., 2009; Mondillo et al., 2011; Boni et al., 2013; Mondillo et al., 2014; Santoro et al., 2014; Mondillo et al., 2015; Paradis et al., 2015; Choulet et al., 2016; Arfè et al., 2017; Balassone et al., 2017).

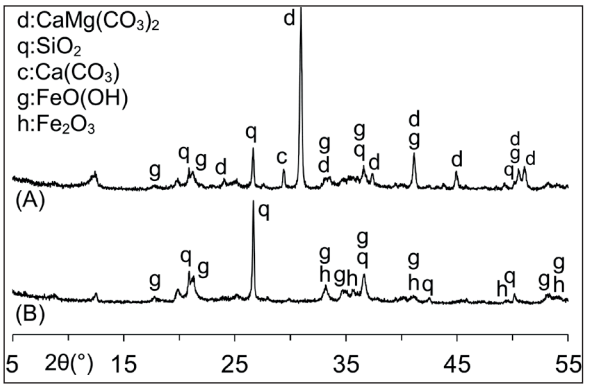

Figure 7. XRD patterns of the undissolved solids obtained after dissolution in (A) 8 M NaOH and (B) 4 M HCl solutions at 298 K

CONCLUSIONS

The dissolution properties of a smithsonite ore sample with dolomite as the main gangue mineral

in NaOH solutions at different temperatures were investigated with the use of different analyses methods. When the ore sample was dissolved in sodium hydroxide solutions, it was found that the dissolution efficiency of zinc continually increased with increasing sodium hydroxide concentrations and the highest zinc dissolution efficiency of 70.7% was obtained after dissolution in 4 M NaOH solution at 298 K. The analyses performed on the undissolved solids obtained after dissolution in sodium hydroxide solutions showed that the smithsonite phase in the studied sample selectively dissolved against main carbonate gangue mineral dolomite in the sample. The separate dissolution experiments performed in sodium hydroxide and hydrochloric acid solutions indicated that, together with the main ore mineral smithsonite, zinc may also be present in the gangue components of the studied ore sample. Finally, together with the results of our previous study (Ehsani et al., 2019), dissolution properties of chemically and mineralogically different two Turkish zinc carbonate ore samples in sodium hydroxide solutions were revealed comparatively in detail and new data were added to the relevant scarce literature. Besides, a new study related with the dissolution of similar smithsonite ore samples in ammoniacal solutions was also initiated for comparison purposes.

ACKNOWLEDGEMENTS

The support of ÖYP research project funding units of Turkish Higher Education Institute is gratefully acknowledged. The authors also thank to Koyuncu Mining Ind.&Trd.Ltd. for supplying the ore sample.

REFERENCES

Abkhoshk, E., Jorjani, E., Al-Harahsheh, M. S., Rashchi, F., Naazeri, M., 2014. Review of the Hydrometallurgical Processing of Non-sulfide Zinc Ores. Hydrometallurgy, 149, 153-167.

Adler, H. H., Kerr, P. F., 1963. Infrared Absorption Frequency Trends for Anhydrous Normal Carbonates. Am. Mineral., 48, 124-137.

Arfè, G., Mondillo, N., Balassone, G., Boni, M., Cappelletti, P., Di Palma, T., 2017. Identification of Zn-bearing Micas and Clays from the Cristal and Mina Grande Zinc Deposits (Bongará province, Amazonas region, northern Peru). Mineral-Basel, 7, 214.

Balassone, G., Nieto, F., Arfè, G., Boni, M., Mondillo, N., 2017. Zn-Clay Minerals in the Skorpion Zn Nonsulfide Deposit (Namibia): Identification and Genetic Clues Revealed by HRTEM and AEM Study. Appl. Clay Sci., 150, 309-322.

Boni, M., Schmidt, P. R., De Wet, J. R., Singleton, J. D., Balassone, G., Mondillo, N., 2009a. Mineralogical Signature of Nonsulfide Zinc Ores at Accha (Peru): A Key for Recovery. Int. J. Miner. Process., 93, 267-277.

Boni, M., Balassone, G., Arseneau, V., Schmidt, P., 2009b. The Nonsulfide Zinc Deposit at Accha (southern Peru): Geological and Mineralogical Characterization. Econ. Geol., 104, 267-289.

Boni, M., Mondillo, N., Balassone, G., Joachimski, M., Coella, A., 2013. Zincian Dolomite Related to Supergene Alteration in the Iglesias Mining District (SW Sardinia). Int. J. Earth. Sci., 102, 61-71.

Borg, G., Kärner, K., Buxton, M., Armstrong, R., Van Der Merwe, S. W., 2003. Geology of the Skorpion Supergene Zinc Deposit, Southern Namibia. Econ. Geol., 98, 749-771.

Choulet, F., Buatier, M., Barbanson, L., Guègan, R., Ennaciri, A., 2016. Zinc-Rich Clays in Supergene Non-Sulfide Zinc Deposits. Miner. Deposita, 51, 467-490.

Coppola, V., Boni, M., Gilg, H. A., Strzelska-Smakowska, B., 2009. Nonsulfide Zinc Deposits in the Silesia-Cracow District, Southern Poland. Miner. Deposita, 44, 559-580.

Cuthbert, F. L., Rowland, R. A., 1947. Differential Thermal Analysis of Some Carbonate Minerals. Am. Mineral., 32, 111-116.

Debiemme-Chouvy, C., Vedel, J., 1991. Supersaturated Zincate Solutions: A study of the Decomposition Kinetics. J. Electrochem. Soc., 138, 2538-2542.

Dhawan, N., Safarzadeh, M. S., Birinci, M., 2011. Kinetics of Hydrochloric Acid Leaching of Smithsonite. Russ. J. Non-Ferr. Met., 52, 209-216.

DPT, 2001. State Planning Organization, Eighth Five-year Development Plan, Mining Specialization Commission Report, Subcommittee of Metal Mines, Lead-Zinc-Cadmium Study Group Report. DPT:2628, OİK:639, Ankara, 85-167 (in Turkish).

Ehsani, I., Ucyildiz, A., Obut, A., 2019. Leaching Behaviour of Zinc from a Smithsonite Ore in Sodium

Hydroxide Solutions. Physicochem. Probl. Mi., 55, 407-416.

Ejtemaei, M., Gharabaghi, M., Irannajad, M., 2014. A Review of Zinc Oxide Mineral Beneficiation Using Flotation Method. Adv. Colloid Interfac., 206, 68-78.

Feng, L., Yang, X., Shen, Q., Xu, M., Jin, B., 2007. Pelletizing and Alkaline Leaching of Powdery Low-Grade Zinc Oxide ores. Hydrometallurgy, 89, 305-310.

Frenay, J., 1985. Leaching of Oxidized Zinc Ores in Various Media. Hydrometallurgy, 15, 243-253.

Frost, R. L., Ding, Z., Ruan, H. D., 2003. Thermal Analysis of Goethite Relevance to Australian İndigenous art. J. Therm. Anal. Calorim., 73, 783.

Ghasemi, S. M. S., Azizi, A., 2017. Investigation of Leaching Kinetics of Zinc from a Low-grade Ore in Organic and Inorganic Acids. J. Min. Environ., 8, 579-591.

Ghasemi, S. M. S., Azizi, A., 2018. Alkaline Leaching of Lead and Zinc by Sodium Hydroxide: Kinetics Modeling. J. Mater. Res. Technol., 7, 118-125.

Gillott, J. E., 1964. Mechanism and Kinetics of Expansion in the Alkali-carbonate Rock Reaction. Can. J. Earth Sci., 1, 121-145.

Grim, R. E., Rowland, R. A., 1942. Differential Thermal Analysis of Clay Minerals and Other Hydrous Materials. Part 1. Am. Mineral., 27, 746-761.

Hitzman, M. W., Reynolds, N. A., Sangster, D. F., Allen, C. R., Carman, C. E., 2003. Classification, Genesis, and Exploration Guides for Nonsulfide Zinc Deposits. Econ. Geol., 98, 685-714.

Hosseini, S. H., Forssberg, E., 2009. Smithsonite Flotation Using Mixed Anionic/Cationic Collector. T. I. Min. Metall. C, 118, 186-190.

Huang, C. K., Kerr, P. F., 1960. Infrared Study of the Carbonate Minerals. Am. Mineral., 45, 311-324.

Hurlbut, C. S. Jr., 1957. Zincian and Plumbian Dolomite from Tsumeb, South-West Africa. Am. Mineral., 42, 798-803.

Ju, S., Motang, T., Shenghai, Y., Yingnian, L., 2005. Dissolution Kinetics of Smithsonite ore in Ammonium Chloride Solution. Hydrometallurgy, 80, 67-74.

Moezzi, A., Cortie, M., McDonagh, A., 2011. Aqueous Pathways for the Formation of Zinc Oxide Nanoparticles. Dalton T., 40, 4871-4878.

Mondillo, N., Boni, M., Balassone, G., Grist, B., 2011. In Search of the Lost Zinc: A Lesson from the Jabali (Yemen) Nonsulfide Zinc Deposit. J. Geochem. Explor., 108, 209-219.

Mondillo, N., Boni, M., Balassone, G., Joachimski, M., Mormone, A., 2014. The Jabali Nonsulfide Zn-Pb-Ag Deposit, Western Yemen. Ore Geol. Rev., 61, 248-267.

Mondillo, N., Nieto, F., Balassone, G., 2015. Micro- and Nano-characterization of Zn-clays in Nonsulfide Supergene Ores of Southern Peru. Am. Mineral., 100, 2484-2496.

Mujahed, S. B., 1966. Electrowinning in Alkaline Medium-Electrolytic Production of Lead and Zinc from an Oxidized Ore from Develi (Kayseri) via Caustic Leaching. MSc Thesis, Middle East Technical Univ.

Paradis, S., Keevil, H., Simandl, G. J., Raudsepp, M., 2015. Carbonate-hosted Nonsulphide Zn-Pb Mineralization of Southern British Columbia, Canada. Miner. Deposita, 50, 923-951.

Rosenberg, P. E., Champness, P. E., 1989. Zincian Dolomites and Associated Carbonates from the Waryński Mine, Poland: An AEM investigation. Am. Mineral., 74, 461-465.

Santoro, L., Boni, M., Rollinson, G. K., Mondillo, N., Balassone, G., Clegg, A. M., 2014. Mineralogical Characterization of the Hakkari nonsulfide Zn(Pb) Deposit (Turkey): The Benefits of QEMSCAN®. Miner. Eng., 69, 29-39.

Uekawa, N., Yamashita, R., Wu, Y. J., Kakegawa, K., 2004. Effect of Alkali Metal Hydroxide on Formation Processes of Zinc Oxide Crystallites from Aqueous Solutions Containing $Zn(OH)_4^{2-}$ ions. Phys. Chem. Chem. Phys., 6, 442-446.

Wang, Y. M., Wainwright, G., 1986. Formation and Decomposition Kinetic Studies of Calcium Zincate in 20 w/o KOH. J. Electrochem. Soc., 133, 1869-1872.

Weir, C. E., Lippincott, E. R., 1961. Infrared Studies of Aragonite, Calcite, and Vaterite Type Structures in the Borates, Carbonates, and Nitrates. J. Res. N.B.S. A Phys. Ch., 65, 173-183.

Whittaker, E. J. W., Żabiński, W., 1981. X-ray Diffraction by Zincian Dolomite. Mineralog. Pol., 12, 15-24.

Zhang, Y., Deng, J., Chen, J., Yu, R., Xing, X., 2013. Leaching of Zinc from Calcined Smithsonite Using Sodium Hydroxide. Hydrometallurgy, 131&132, 89-92.

Zhao, Y., Stanforth, R., 2000. Production of Zn Powder by Alkaline Treatment of Smithsonite Zn-Pb Ores. Hydrometallurgy, 56, 237-249.